# Longshore sediment transport at Golden Sands (Bulgaria)*

OCEANOLOGIA, 48 (3), 2006.
pp. 413–432.



**KEYWORDS**
Golden Sands
Sediment transport
Wave refraction
and diffraction
Offshore wave climate

Hristo Nikolov[1]
Ekaterina Trifonova[1]
Zhivelina Cherneva[1]
Rafał Ostrowski[2,*]
Marek Skaja[2]
Marek Szmytkiewicz[2]

[1] Institute of Oceanology,
Bulgarian Academy of Sciences,
(IO BAS),
PO Box 152, 9000 Varna, Bulgaria

[2] Institute of Hydroengineering,
Polish Academy of Sciences,
(IBW PAN),
Kościerska 7, PL–80–328 Gdańsk, Poland;

e-mail: rafi@ibwpan.gda.pl;

*corresponding author

Received 18 March 2006, revised 6 September 2006, accepted 11 September 2006.

**Abstract**

The paper presents the results of studies on the qualitative and quantitative features of the littoral drift at Golden Sands (Bulgaria), carried out jointly

* The study was funded by the Ministry of Science and Higher Education, Poland, under programme 2 IBW PAN, and by the IO BAS statutory research programme. The activities relating to this study were also supported within the joint Polish-Bulgarian cooperation project by the Polish Academy of Sciences and the Bulgarian Academy of Sciences, which are hereby gratefully acknowledged.

by Polish and Bulgarian researchers. The mathematical modelling of physical coastal processes took wave transformation (wave diffraction and refraction; the effects of shoaling and wave breaking) and longshore sediment transport into account. The computations were carried out for the mean statistical annual wave climate, determined on the basis of IO BAS wave data, simulated using the WAM method from long-term Black Sea wind data. The results of sediment transport computations clearly show that its direction off the Golden Sands shore is from north to south.

## 1. Introduction

Coastal zones are of great economic importance in all countries having access to the sea. Sandy beaches make up one third of the total length of the Bulgarian Black Sea coast (the rest is rocky), while on the Polish Baltic Sea shore sandy beaches and dunes constitute about 80% of the coast (the other shore sections consist of sandy-clayey cliffs). In both countries, a considerable recreational and tourist potential is concentrated on the coast. Coastal engineering problems have therefore been a topic of many investigations and case studies in Bulgaria and Poland. In some of them, the Polish and Bulgarian researchers from the Institute of Hydroengineering of the Polish Academy of Sciences (IBW PAN) and the Institute of Oceanology of the Bulgarian Academy of Sciences (IO BAS) respectively, have linked their efforts to find solutions to practical coastal engineering problems.

Different natural factors influence coastal zone development, and the action of these factors changes during the long-term evolution of the Earth's climate. At each stage of a coastal zone's development, the dynamic equilibrium results in the quasi-constant shape of the cross-shore profile and in the quasi-constant location of the shoreline. Nevertheless, human intervention (disturbance) in coastal zone processes can disrupt this state of equilibrium.

In order to assess the influence of man-made structures on coastal dynamics, the features and parameters of the natural (undisturbed) hydrodynamics and lithodynamics should be determined: in particular, the wave climate, wave transformation patterns, wave-driven flow velocities and longshore sediment transport rates ought to be calculated. Once existing processes have been identified qualitatively and quantitatively, attempts can then be made to assess potential anthropogenic impacts on the seashore (see Nikolov & Keremedchiev 1993, Szmytkiewicz et al. 2000, Nikolov & Mutafova 2001).

The shore at Golden Sands, located on the west coast of the Black Sea (see Fig. 1), is in a state of a relative equilibrium, with a slight tendency to local erosion effects (see Dachev & Nikolov 1977). Long-term observations, including the shoreline's response to the erection of (small)

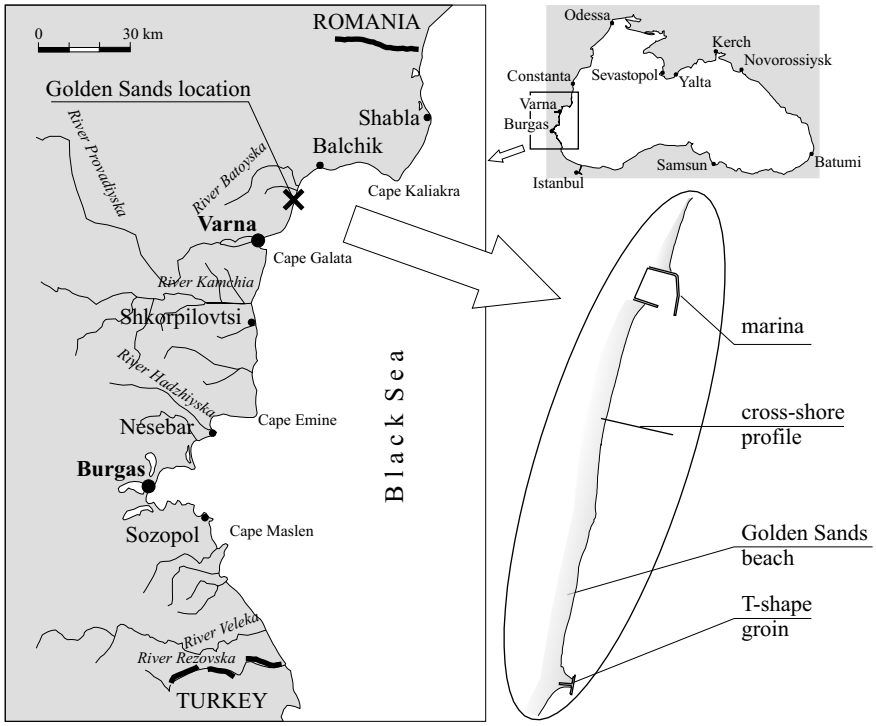


**Fig. 1.** Location of Golden Sands on the Black Sea coast

coastal structures, namely, the accumulation of sand to the south of a marina and the filling of both (southern and northern) 'pockets' of a T-shaped groyne, lead to the preliminary qualitative conclusion that the long-term net sediment transport along this section of the shore takes place in a northerly direction. The results of previous investigations of longshore sediment transport along this section of the coast (Shuysky & Popov 1975, Dachev & Cherneva 1979, Filippov 1988) have not been completely unequivocal as regards the direction of this transport. Calculating the longshore transport along the Bulgarian coast was first attempted by Shuysky & Popov (1975), according to whom the longshore sediment transport in the area of investigation was directed from north to south. Dachev & Cherneva (1979) also carried out a meticulous study of this longshore sediment transport: they assessed the so-called longshore fluxes of wave energy using an approach proposed by Longinov (1966) for the north Bulgarian coast. These energy fluxes were assumed to represent the potential rates of longshore sediment transport. The results obtained by Filippov (1988), concerning the longshore transport direction of suspended sediments, tally with those of Shuysky & Popov (1975). These three studies clearly implied

that the motion of sand along the Bulgarian coast was mostly directed southwards. Exceptionally, in the region of Golden Sands, according to Dachev & Cherneva (1979), the resultant movement of sediments was in a northerly direction. The necessity of new, in-depth studies of natural processes at Golden Sands arose from the qualitative discrepancies between the sediment-filled 'pockets' at two coastal structures, the assessments of previous investigators, not to mention the exceptional significance of the 'Golden Sands' tourist complex for the Bulgarian recreational industry.

Sediment transport parameters, as well as the qualitative and quantitative features of coastal morphodynamics, are highly dependent on the wave climate (see e.g. Filippov 1988, Pruszak et al. 2000). This wave climate is shaped by a set of boundary conditions: the annual distribution (frequencies) of wind speed and direction, the wind fetch (dimensions of a sea), and the bathymetry. Moreover, the nearshore wave climate can be substantially modified (with respect to the offshore wave climate) as a result of wave refraction and diffraction. In particular, on an indented coastline (with capes and bays), wave diffraction can play a significant role and local peculiarities in the nearshore hydrodynamics can occur.

No detailed, process-based modelling of coastal hydrodynamic and lithodynamic phenomena has yet been carried out for Golden Sands. The present study attempted to reproduce the entire sequence of these phenomena: wave transformation from the offshore region to the nearshore zone (including the surf zone), generation of the longshore wave-driven current, and longshore sediment transport. This was achieved using the fully deterministic modelling approach, with the input deepwater waves simulated from wind parameters over the entire Black Sea.

The modelling procedures were carried out using theoretical concepts developed in the form of scientific software at IBW PAN and IO BAS, as well as the licensed commercial software (UNIBEST-LT, Delft Hydraulics) made available to IBW PAN for research purposes in the early 1990s. Since the present paper is a kind of case study, the modelling theoretical background is described in brief. Full details of the theories and concepts involved are provided in the references.

## 2. Wave climate

The deepwater wave parameters were previously computed with the use of the WAM method at IO BAS.

WAM C4 (Wave Model), a third-generation ocean wave prediction model, uses a common propagation system in which energy conservation takes place without any restrictions placed on the wave spectrum. The atmospheric pressure fields, provided by the global baric re-analysis ECMWF,

are used as input data for the modelling. As a result of model work, significant wave heights $H_s$, wave directions $\theta$ and wave peak periods $T_p$ are calculated for every point of the grid and every moment of time. For the Black Sea region, the space mesh is $0.5 \times 1.0°$.

The computations were carried out for a deepwater point (43°30′N, 29°E; 70 m depth, about 32 km east of Cape Shabla) on the basis of atmospheric pressure fields for the years 1958–98. This period (41 years) was deemed satisfactory for determining the representative wave climate in the mean statistical year. The results of modelling were grouped into 1204 sets of $H_s - \theta$ space, from which averaged values of $H_s$, $\theta$ and $T_p$ were determined.

The spatially averaged shoreline at Golden Sands has an azimuth of about 19°. The line perpendicular to the shore has an azimuth of 109°, with respect to which the wave rays constitute the angles $\theta$ ($\theta = 0°$ denotes wave incidence perpendicular to the shore, while $\theta = \pm 90°$ implies deepwater waves moving parallel to the coastline)[1]. The parameters of waves propagating from seaward directions (in the azimuth range 19°–199°), i.e. the significant wave height $H_s$, the wave peak period $T_p$, the azimuth of wave approach $Az$, wave ray angles $\theta$ and duration $t$, obtained by the statistical analysis, are given in Table 1 (durations less than 0.1 day were neglected).

Table 1 shows that the waves come predominantly from the northern sector. Such a situation lasts for about 43% of the mean statistical year, while for 19% of this year the waves come from the southern sector. For only 38% of the mean statistical year, there are no waves or they are directed seawards.

To obtain the representative wave climate off the Golden Sands coastal section at 20 m depth, the wave refraction model developed at IO BAS (Trifonova 2005) was used. This model comprises the numerical solution to the wave vector conservation equation. Wave velocity is presented as a function of depth and period, and wave heights are defined from the wave energy balance equation. In the present study, a two-dimensional variant of the model was applied. The results were assigned to 66 groups in $H_s - \theta$ space. Fig. 2 shows the distribution of wave attack duration for every group in $H_s - \theta$ space for the point at 20 m depth off Golden Sands.

The data for both the deepwater point (80 m depth) and the point off Golden Sands (20 m depth) show that the resultant deepwater longshore wave energy flux is directed southwards. This implies that the longshore sediment transport in the coastal zone is also directed southwards.

[1]Positive values stand for waves coming from the N–E sector (the left-hand side of an observer looking seawards), while negative values denote waves coming from the E–S sector (the right-hand side of an observer looking seawards).

**Table 1.** Representative offshore (for $h = 70$ m) wave climate at Golden Sands in the mean statistical year

| Wind direction | $H_s$ [m] | $T_p$ [s] | $Az$ [°] | $\theta$ [°] | $t$ [days] |
|---|---|---|---|---|---|
| 1 | 2 | 3 | 4 | 5 | 6 |
| NNE | 1.3 | 5.8 | 20.0 | 89.0 | 5.1 |
| 10% | 2.0 | 6.8 | 20.0 | 89.0 | 2.7 |
| | 0.7 | 4.7 | 20.2 | 88.8 | 5.8 |
| | 2.8 | 7.8 | 20.9 | 88.1 | 1.2 |
| | 4.1 | 8.8 | 22.1 | 86.9 | 0.2 |
| | 4.7 | 9.6 | 29.1 | 79.9 | 0.1 |
| | 5.6 | 10.2 | 29.6 | 79.4 | 0.1 |
| | 2.0 | 6.9 | 29.7 | 79.3 | 2.8 |
| | 2.8 | 7.9 | 29.9 | 79.1 | 1.6 |
| | 0.7 | 5.1 | 30.0 | 79.0 | 10.2 |
| | 1.3 | 6.0 | 30.0 | 79.0 | 6.0 |
| | 3.7 | 8.9 | 30.3 | 78.7 | 0.5 |
| NE | 2.8 | 7.9 | 38.9 | 70.1 | 1.7 |
| 13% | 0.7 | 5.1 | 39.0 | 70.0 | 15.7 |
| | 2.0 | 6.9 | 39.1 | 69.9 | 3.3 |
| | 3.7 | 8.8 | 39.1 | 69.9 | 0.7 |
| | 1.3 | 6.0 | 39.3 | 69.7 | 7.8 |
| | 5.6 | 10.2 | 39.6 | 69.4 | 0.1 |
| | 4.6 | 9.5 | 40.0 | 69.0 | 0.4 |
| | 3.7 | 9.0 | 49.2 | 59.8 | 0.4 |
| | 1.3 | 6.0 | 49.3 | 59.7 | 4.9 |
| | 0.7 | 4.9 | 49.5 | 59.5 | 9.8 |
| | 2.0 | 7.0 | 49.6 | 59.4 | 1.8 |
| | 4.6 | 9.6 | 49.6 | 59.4 | 0.2 |
| | 2.8 | 8.0 | 50.0 | 59.0 | 1.1 |
| | 5.6 | 10.4 | 50.5 | 58.5 | 0.1 |
| ENE | 4.9 | 9.9 | 58.8 | 50.2 | 0.2 |
| 10% | 2.8 | 8.1 | 59.1 | 49.9 | 0.9 |
| | 1.3 | 6.3 | 59.3 | 49.7 | 5.4 |
| | 2.0 | 7.1 | 59.3 | 49.7 | 1.9 |
| | 0.7 | 5.0 | 59.3 | 49.7 | 11.0 |
| | 3.7 | 9.1 | 59.7 | 49.3 | 0.4 |
| | 5.3 | 10.5 | 69.2 | 39.8 | 0.1 |
| | 3.7 | 8.9 | 69.3 | 39.7 | 0.3 |
| | 1.3 | 6.8 | 69.4 | 39.6 | 4.1 |
| | 0.7 | 5.6 | 69.5 | 39.5 | 9.0 |
| | 2.8 | 8.4 | 69.8 | 39.2 | 0.7 |
| | 2.0 | 7.5 | 69.9 | 39.1 | 1.5 |

**Table 1.** (*continued*)

| 1 | 2 | 3 | 4 | 5 | 6 |
|---|---|---|---|---|---|
| E | 1.3 | 7.0 | 79.1 | 29.9 | 4.8 |
| 14% | 0.7 | 6.0 | 79.2 | 29.8 | 13.2 |
| | 2.0 | 7.6 | 79.4 | 29.6 | 1.5 |
| | 3.7 | 9.2 | 79.9 | 29.1 | 0.4 |
| | 2.8 | 8.4 | 80.0 | 29.0 | 0.8 |
| | 4.7 | 10.2 | 80.9 | 28.1 | 0.1 |
| | 6.0 | 11.1 | 81.7 | 27.3 | 0.1 |
| | 4.5 | 9.8 | 88.0 | 21.0 | 0.1 |
| | 0.7 | 5.6 | 89.2 | 19.8 | 9.6 |
| | 2.0 | 7.5 | 89.4 | 19.6 | 1.1 |
| | 3.7 | 9.1 | 89.6 | 19.4 | 0.3 |
| | 6.0 | 11.0 | 89.6 | 19.4 | 0.1 |
| | 1.3 | 6.6 | 89.9 | 19.1 | 3.6 |
| | 2.8 | 8.4 | 89.9 | 19.1 | 0.7 |
| | 5.4 | 10.3 | 97.1 | 11.9 | 0.1 |
| | 2.8 | 8.2 | 98.3 | 10.8 | 0.3 |
| | 2.0 | 7.4 | 98.7 | 10.3 | 0.8 |
| | 1.3 | 6.6 | 99.0 | 10.0 | 4.0 |
| | 3.8 | 9.1 | 99.2 | 9.8 | 0.1 |
| | 0.7 | 5.3 | 99.3 | 9.7 | 9.8 |
| ESE | 1.3 | 6.3 | 108.6 | 0.4 | 1.6 |
| 3% | 0.7 | 5.2 | 109.0 | 0.0 | 5.8 |
| | 2.2 | 7.0 | 109.0 | 0.0 | 0.2 |
| | 2.0 | 6.3 | 118.8 | −9.8 | 0.1 |
| | 0.7 | 4.8 | 118.8 | −9.8 | 3.4 |
| | 1.3 | 5.7 | 119.5 | −10.5 | 0.6 |
| SE | 0.7 | 4.4 | 129.5 | −20.5 | 1.9 |
| 1% | 1.7 | 6.3 | 130.3 | −21.3 | 0.4 |
| | 0.7 | 4.2 | 139.8 | −30.8 | 2.4 |
| | 1.6 | 5.7 | 140.8 | −31.8 | 0.4 |
| SSE | 1.6 | 5.5 | 149.5 | −40.5 | 0.4 |
| 2% | 0.7 | 4.1 | 149.8 | −40.8 | 2.2 |
| | 1.2 | 5.0 | 159.4 | −50.4 | 0.5 |
| | 0.7 | 4.1 | 159.5 | −50.5 | 3.2 |
| | 2.0 | 6.2 | 160.6 | −51.6 | 0.1 |
| S | 1.3 | 5.3 | 169.9 | −60.9 | 0.8 |
| 9% | 0.7 | 4.2 | 170.0 | −61.0 | 3.9 |
| | 2.1 | 6.4 | 170.4 | −61.4 | 0.2 |
| | 0.7 | 4.4 | 180.0 | −71.0 | 8.4 |
| | 1.3 | 5.5 | 180.6 | −71.6 | 2.5 |

**Table 1.** (*continued*)

| 1 | 2 | 3 | 4 | 5 | 6 |
|---|---|---|---|---|---|
| S | 2.0 | 6.4 | 180.9 | −71.9 | 0.5 |
| 9% | 3.0 | 7.6 | 181.0 | −72.0 | 0.2 |
| | 0.7 | 4.4 | 189.2 | −80.2 | 7.2 |
| | 2.0 | 6.6 | 189.6 | −80.6 | 1.0 |
| | 1.3 | 5.6 | 189.7 | −80.7 | 3.7 |
| | 3.0 | 7.6 | 190.4 | −81.4 | 0.4 |
| | 2.9 | 7.5 | 196.6 | −87.6 | 0.2 |
| | 2.2 | 6.7 | 197.8 | −88.8 | 0.4 |
| | 1.3 | 5.6 | 198.0 | −89.0 | 1.9 |

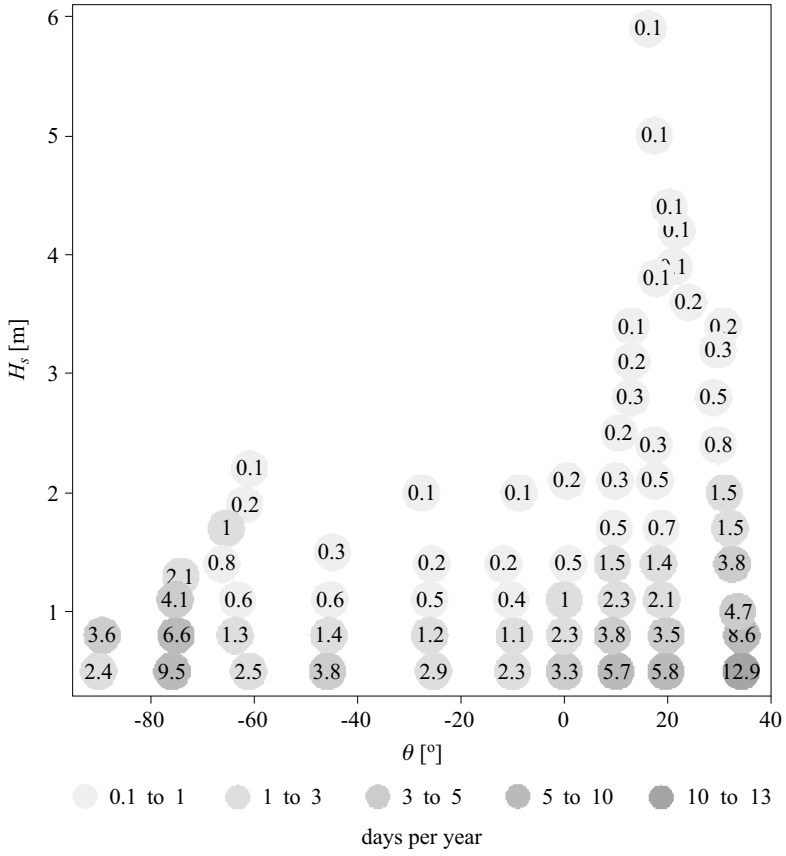


**Fig. 2.** Duration of wave attack in the statistical year

The findings concerning offshore wave directions near the coast in question are in agreement with results of the study by Cherneva et al. (2003) and Ozhan et al. (2005).

## 3. Wave transformation and longshore currents

Wave transformation and the generation of wave-induced flow on the typical cross-shore profile at Golden Sands were numerically simulated using the SAND94 numerical package (developed at IBW PAN) and the UNIBEST-LT software (Delft Hydraulics). The modelling approach is now briefly described.

Following Battjes & Janssen (1978), it is assumed in the computations of wave motion that waves are random and that their heights in the entire coastal zone can be described by a Rayleigh distribution. On the basis of his experimental investigations and other available data, Szmytkiewicz (2002a,b) deduced that this rough assumption leads to inaccuracies of no more than 10% in the determination of wave height in a nearshore zone. The so-called 'roller effect' is also taken into consideration. This means that the lag between wave breaking and the appearance of currents is represented in the equations of momentum and energy by a rotating roller of water, located on the crest of the breaking wave. According to this concept, the wave energy lost during wave breaking is initially transferred to roller induction, after which the water flows appear.

In the wave-current computational framework, in which wave refraction is assumed to be linear, the variability in wave angle approach is calculated from Snell's law, while the wave number $k$ is determined from the dispersion relationship for the linear wave theory. Assuming that there are no wave reflections from the shore and that there is no interaction between waves and current, the wave height $H$ is computed from the energy flux conservation equation.

In the longshore current model, with the assumption of approximately parallel isobaths and the Boussinesq hypothesis regarding turbulent shear stresses, the depth-invariable velocity is obtained, averaged over the wave period. This velocity is a function of offshore distance. In the modelling system, the gradient of the wave radiation stress $S_{xy}$ component is the active (driving) force causing water motion, whereas the turbulent stresses and bottom friction are the drag forces. The driving factor $S_{xy}$ is calculated as a function of wave energy dissipation.

The model of wave transformation and longshore current is capable of correctly describing the velocity distribution over a cross-shore profile for multiple wave breaking. The solution depends closely on the assumed turbulent viscosity $\nu_T$ and the bottom friction coefficient $f$.

The quantity $f$ in most longshore current models is determined on the basis of measurements and is assumed constant for the entire coastal zone. For practical calculations of longshore current velocities, the friction

coefficient $f$ should be determined for the hydro- and lithodynamic conditions specific to the analysed area.

The determination of the kinematic turbulent viscosity $\nu_T$ is a serious and extremely complex problem. A number of approaches are proposed in the literature, e.g. by Szmytkiewicz (2002b), who has discussed and tested a few of them, including the best-known ones by Thornton (1970) and Bosboom et al. (1997). In Thornton's model, $\nu_T$ is calculated as a function of orbital velocity near the bottom; in Bosboom's approach this quantity is determined as a function of wave energy dissipation and wave height. The average value of the turbulent viscosity in the surf zone has been estimated at $\nu_T \approx 0.02$ m$^2$ s$^{-1}$.

Example wave transformations and longshore currents computed for an offshore wave with parameters $H_s = 1.1$ m, $T_p = 6.7$ s and $\theta = 39.4°$ are plotted in Fig. 3.

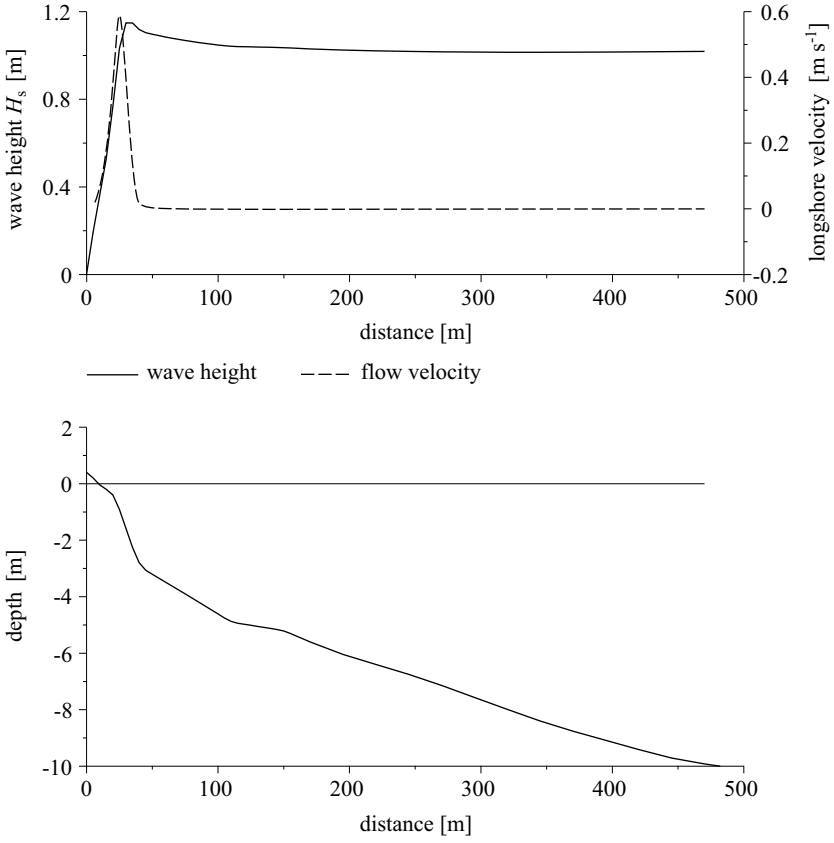


**Fig. 3.** Examples of wave heights and longshore current velocities calculated for the nearshore part of the cross-shore profile at Golden Sands; $H_s = 1.1$ m, $T_p = 6.7$ s and $\theta = 39.4°$

## 4. Sediment transport

Longshore sediment transport rates were computed using the theoretical models of Bijker (1971) and Van Rijn (1993), as well as the model of Bailard (1981), all of which are available in the UNIBEST-LT (1993) software.

In the Bijker model, the bedload transport is determined as a function of longshore flow velocity and wave nearbed free-stream velocity, whereas the suspended load rate is calculated on the basis of the bedload rate. In this approach, the sediment is represented by two characteristic grain diameters: $d_{50}$ (the median grain size diameter) and $d_{90}$. However, Bijker's formula is reported to overestimate the sand motion for low transport capacities.

Bailard's formula is based on an energetics approach, originally suggested by Bagnold for unidirectional flow. The bedload formulation originates from a force balance between pressure and shear stress gradients in the moving sediment layer on the one hand and gravitational forces on the other. The suspended load formulation is based on an assumed linear relation between the energy produced by the sediment-free-stream and the power needed to keep sediment particles in suspension. There are two so-called efficiency factors in the model – one for bottom transport and a second one for suspended transport. These quantities must be assumed on the basis of some knowledge of the sediment transport rate at the site under consideration.

The transport formulation proposed by Van Rijn is similar to Bijker's approach, but takes account of bed shear stresses in a more detailed way. In particular, current-related bottom roughness and wave-related bottom roughness are introduced as functions of the height of bed forms (ripples). In the class of engineering models, Van Rijn's model is regarded as a relatively accurate method.

The sediment parameters in the models were assumed to be $d_{50} = 0.24$ mm, $d_{90} = 0.35$ mm and the settling velocity of grains $w_s = 0.03$ m s$^{-1}$. Sediment transport rates were calculated for all hydrodynamic conditions of the mean statistical year. Example results are depicted in Fig. 4, which shows that Bailard's model in this case yields much smaller sediment transport rates than the approaches of Bijker and Van Rijn (the results by which are quite similar to each other).

Next, all the longshore sediment transport rates were integrated over the cross-shore profile, as well as over the year (accounting for the duration of the consecutive events), yielding the total (net) annual volume of sediment transport. The calculations for the mean statistical year yielded results in the following ranges[2]:

[2]Depending on the assumed values of constants, coefficients and tuning parameters of the models.

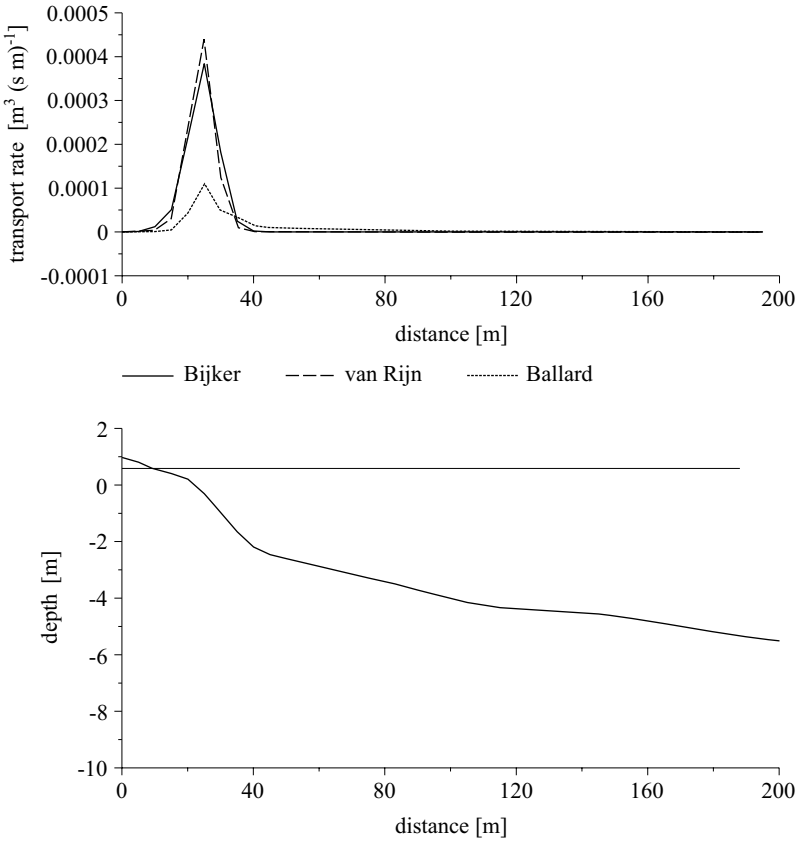


**Fig. 4.** Examples of longshore sediment transport rates calculated for the nearshore part of the cross-shore profile at Golden Sands; $H_s = 1.1$ m, $T_p = 6.7$ s and $\theta = 39.4°$

- Bailard – from 46 000 to 56 000 $m^3\ yr^{-1}$;
- Bijker – from 62 000 to 73 000 $m^3\ yr^{-1}$;
- Van Rijn – from 68 000 to 80 000 $m^3\ yr^{-1}$.

The positive values of the above results imply that the net longshore sand transport is directed from N to S. The computations taking into account only waves from the S–E sector show that the S–N longshore sediment transport is very small:

- Bailard – 1000 $m^3\ yr^{-1}$,
- Bijker – 3000 $m^3\ yr^{-1}$,
- Van Rijn – 2000 $m^3\ yr^{-1}$.

The results of these calculations show that southward sediment transport clearly predominates over the northward transport; the accumulation of

sand to the south of the marina does not confirm this, however. Short-term morphological data are available for the Golden Sands region, comprising the shoreline position measured before and after the erection of the marina structures in 1979 (a groyne perpendicular to the shoreline) and in 1983 (a breakwater parallel to the shoreline). The measurements reveal the accumulation of sediment on the southern side of the groyne immediately after its construction (see Fig. 5).

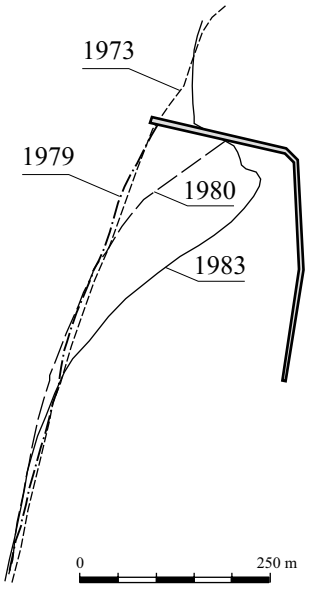


**Fig. 5.** Shoreline evolution after the construction of the marina at Golden Sands

In 1976 a T-shaped groyne was constructed at the southern end of Golden Sands. After that, accretion of the sea shore took place on both sides of the groyne (see Fig. 6). The records of changes in the shoreline position close to the groyne prove that accumulation took place on the north side of the structure as a result of north-south longshore transport brought about by waves from the NE, as well as on the south side due to waves from the SE. Thus, it can be seen distinctly that two longshore sediment fluxes coexist in this region, which are related to the two dominant directions of wind and waves.

The sizes and positions of both structures predetermine their different impact on coastal processes. One glance at their layouts identifies obvious differences in their shapes and sizes. This, in turn, helps to define their different impacts on accumulation processes and the dynamics of the shoreline position and underwater coastal slope.

The larger size and Γ-shape of the marina to a great extent protects the longer sector of the beach at Golden Sands; therefore, the dominant waves

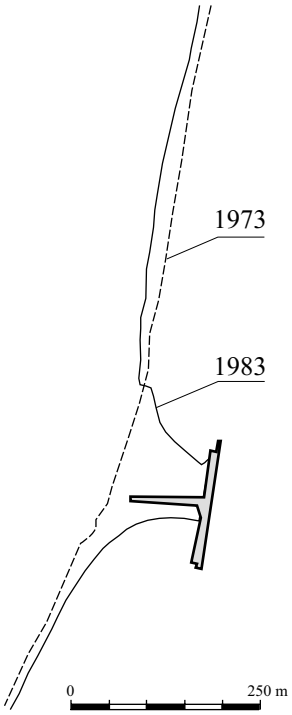


**Fig. 6.** Shoreline evolution after the construction of a T-shaped groyne at Golden Sands

from the NE, giving rise to a southward longshore energy flux, directly affect the shorter beach sector. The smaller size of the T-shaped groyne, situated at the south end of the beach, accordingly protects the shorter beach sector, while waves from the SE directly affect the longer beach segment. At this point it should be recalled that the waves from the NE have a considerably higher energy. In winter, therefore, some of the sediment is washed out of the shoreline and is deposited along the underwater slope at depths from 2.5–3 m to 4–5 m; as a result, much less sediment is accumulated in the 'pocket' of the T-shaped groyne.

During summer, waves from the south are generally dominant. The energy of these waves is much lower, but they affect the longer beach segment, not protected by the T-shaped groyne. The summer wave motion thus causes the sediment to move back from its place of deposition towards the shore. This lithodynamic process, however, applies to sand accumulated at depths of less than 3 m, whereas sediment deposited at 4–5 m remains there. In addition, the longshore sediment transport in summer, affecting the nearshore zone from the shoreline to depths of 2.5–3 m, results in the accumulation of sand to the south of the marina. This material is trapped between the marina breakwater and the marina groyne, and so is unlikely to move under any wave conditions.

Studies of the wind-wave climate and its impact on Black Sea coastal processes, carried out by a number of Bulgarian and foreign scientists, tally with the results obtained in the present model study. Only Dachev & Cherneva (1979) found the longshore wave energy flux to be directed northwards. This result, however, was obtained by applying the methodology developed for an open, straight coast to the deeply indented Bulgarian Black Sea coast, without any consideration for refraction phenomena.

The larger amount of sand accumulated to the south of the Γ-shaped marina can be explained by the different degrees of protection offered by the groynes, the different lengths of protected shoreline, and the different regimes of wave energy impact controlling sediment removal and transport on both beach and underwater coastal slope, but in the absence of any significant northward longshore sediment transport.

## 5. Wave diffraction at Cape Kaliakra

In order to clarify the shoreline dynamics, a more detailed analysis of the nearshore wave climate at Golden Sands was undertaken. In particular, the wave input was revised thoroughly in the specific context of the site's location, the north side of which is sheltered to a significant extent by Cape Kaliakra (see Fig. 7). This means that, as a result of wave diffraction at the cape, a considerable part of the deepwater wave climate (on the open sea, far offshore) does not apply to the coastal zone of Golden Sands.

Wave diffraction is a process in wave propagation that in some cases can be even more important than refraction and shoaling. Conventionally, the diffracted wave height $H$ is calculated from the following simple formula:

$$H = K_d H_i, \tag{1}$$

where $H_i$ is the incident wave height (before diffraction) and $K_d$ is the diffraction coefficient. $K_d$ depends on the distance from the diffracting point $r$, the location of the sought-after diffracted wave in the lee of the cape, as well as the period $T$ (or length $L$) and direction of the incident wave. In this particular case, Cape Kaliakra is the diffracting point, while the solution of diffracted wave is sought at Golden Sands, about 30 km from the cape. The line from Cape Kaliakra to Golden Sands makes an angle of 40° with the locally averaged coastline position to the west of Cape Kaliakra (see Fig. 7).

The diffraction coefficients $K_d$ in the lee of the structure (here: the cape) include the effects of the diffracted incident wave and the much smaller diffracted wave reflected from the structure (here: the shore). The solution to this problem has been published, e.g., in the Shore Protection Manual (1984). The results are given as plots for $r/L$ ranging from 0 to 10 and for

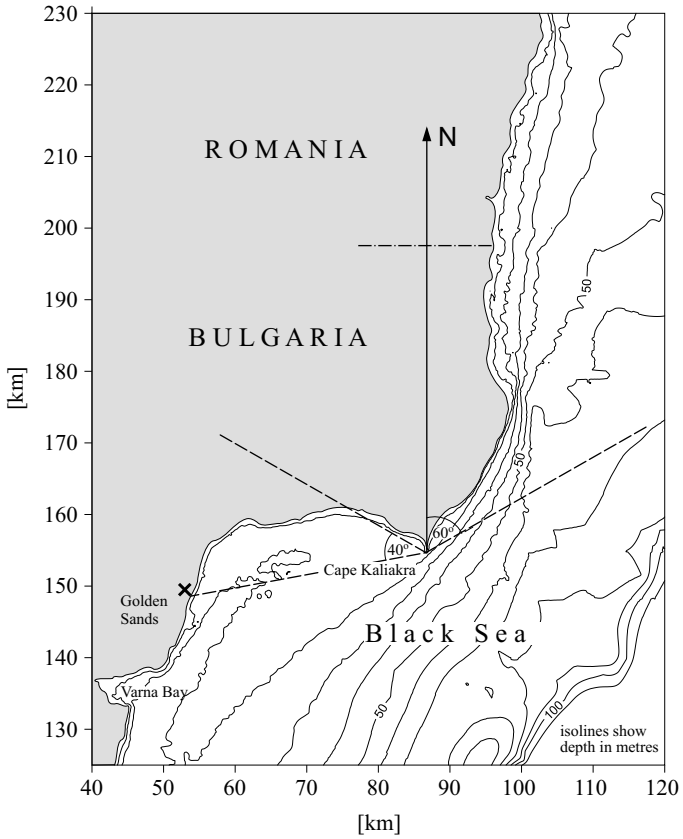


**Fig. 7.** Golden Sands sheltered by Cape Kaliakra: view for wave diffraction analysis

wave approach angles varying by 15-degree intervals from 15° to 180°. In all the plots, the value of $K_d$ along a line in the lee of the diffracting point in the direction of the approaching wave is approximately 0.5. This implies that for each approach angle, the height of a wave in the 'shadow' of the cape is at least half that of the incident wave.

From the analysis of the diffraction patterns carried out in the aforementioned graphs, it appears that for offshore waves coming from the N (0° azimuth) and NE (45° azimuth) the diffraction coefficient $K_d$ at Golden Sands does not exceed 0.1–0.15. Even for an incident wave ray with an azimuth of 60°, $K_d$ lies below 0.2. This implies that the height of the deepwater waves approaching Cape Kaliakra from the above sector ($< 0°$; $60° >$) is at least 5 times smaller at Golden Sands (in the deep water, beyond the nearshore zone). Used as an input in the modelling of wave shoaling/refraction and sediment transport, these waves make a very small contribution to the net sediment transport rate.

In view of the above considerations, the calculations of sediment transport rates were repeated with a limited wave data set (waves with a 0–60° azimuth were removed from the wave input). The following additional model runs were also carried out:

- with the so-called zone of active sediment motion restricted to 200 m only (Nikolov 1981), representing the probable deficit of non-cohesive sediments at Golden Sands;
- by rotating the spatially averaged shoreline at Golden Sands by +10° (right) and −10° (left).

The representative cross-shore profile (shown in Fig. 3) is assumed perpendicular to the coastline. Determining the locally averaged shoreline position may be ambiguous, as it depends on the length of the coastal sector over which the shoreline is approximated by a straight line. The computations with the rotated shoreline were carried out to check the quantitative influence of shoreline position on sediment transport rates.

The annual sand transport volumes computed for the mean statistical year (net – resultant for both longshore directions, as well as gross – from N and S) are presented in Table 2.

**Table 2.** Sediment transport volumes [thousands of $m^3$] at Golden Sands computed for the mean statistical year, taking account of wave diffraction at Cape Kaliakra

| Model | Active sand motion zone of unlimited width | | | Active sand motion zone of width limited to 200 m | | |
|---|---|---|---|---|---|---|
| | Total transport | Transport from N | Transport from S | Unmoved shoreline | Shoreline rotated by +10° | Shoreline rotated by −10° |
| Bailard | 34 | 36 | −2 | 14 | 19 | 7 |
| Bijker | 50 | 55 | −5 | 35 | 45 | 21 |
| Van Rijn | 41 | 46 | −5 | 32 | 47 | 16 |

The results shown in Table 2 depict the predominance of longshore sediment transport directed southwards. This confirms (although qualitatively) the earlier findings arrived at on the basis of modelling results obtained by the use of non-diffracted waves. For the waves diffracted at Cape Kaliakra, even for a shoreline rotated by −10°, the net sand motion in the mean statistical year still takes place from N to S, in accordance with the general tendency observed on most Bulgarian shores.

## 6. Concluding Remarks

As a result of theoretical considerations and numerical modelling, some findings have been produced that have shed more light on the hydrodynamic

and lithodynamic processes occurring in the coastal zone of the Golden Sands region. The detailed conclusions are summarised below.

- The deepwater wave parameters, previously computed at IO BAS with the use of the WAM method on the basis of the atmospheric pressure fields assessed for the years 1958–98, were used to determine the representative wave climate in the mean statistical year. It was found that the waves arrive predominantly from the N–E sector. Such a situation lasts for about 43% of the mean statistical year, while for 19% of this year the waves come from the S–E sector. For 38% of the mean statistical year, no waves directed onshore occur.
- The longshore sediment transport rates were computed using the theoretical models of Bailard (1981), Bijker (1971) and Van Rijn (1993), all available in the UNIBEST (Delft Hydraulics) software. The results obtained for all hydrodynamic conditions of the mean statistical year were then integrated over the cross-shore profile, as well as over the year (accounting for the duration of the consecutive events), yielding the total resultant (net) annual volume of sediment transport: from a minimum of 46 000 $m^3$ obtained with Bailard's model to a maximum of 80 000 $m^3$ with Van Rijn's model.
- For the modified wave input, taking account of wave diffraction at Cape Kaliakra, the computed annual net sediment transport rates at Golden Sands vary from 7000 $m^3$ (Bailard's model, shoreline rotated by –10°, zone of active sand motion limited to 200 m) to 50 000 $m^3$ (Bijker's model, unmoved shoreline, unlimited zone of active sand motion). These values appear to provide ultimate confirmation that the resultant, long-term, longshore sediment transport at Golden Sands is directed southwards.
- The above results provide interesting information in the context of some previous theoretical assessments. In part, however, they do not conform to available coastal morphodynamic data, namely the data on sediment accumulation at the Golden Sands marina, where measurements reveal local short-term accumulation of sediments to the south of the marina and at the T-shaped groyne, also constructed in Golden Sands, where accumulation takes place on both sides of the structure. The accumulation at the T-shaped groyne is due mostly to two coexisting, seasonally variable sediment fluxes, generated by NE and SE winds in winter and summer respectively.
- The greater amount of sand accumulated to the south of the Γ-shaped marina in comparison to shore accretion at the T-shaped groyne results from the different degrees of protection offered by the

structures, the different lengths of protected shore sectors, as well as the different schemes of wave energy impact controlling erosive and accumulative processes, but in the absence of any resultant northward longshore sediment transport.

## References

Bailard J. A., 1981, *An energetics total load sediment transport model for a plane sloping beach*, J. Geophys. Res., 86 (C11), 10938–10954.

Battjes J. A., Janssen J. P. F. M., 1978, *Energy loss and set-up due to breaking of random waves*, Proc. 16th ICCE, Vol. 1, 569–587.

Bijker E. W., 1971, *Longshore transport computations*, J. Waterway. Harbour. Coast. Eng. Div.-ASCE, 97 (WW4), 687–701.

Bosboom J., Aarninkhof S. G. J., Reniers A. J. H. M., Reoelvink J. A., Walstra D. J. R., 1997, *Overview of model formulations*, Delft Hydraul. Rep. No H2305.42.

Cherneva Z., Valchev N., Petrova P., Andreeva N., Valcheva, N., 2003, *Offshore wind wave distribution in the Bulgarian part of the Black Sea*, Proc. Inst. Oceanol. BAS, Vol. 4, 10–18, (in Bulgarian).

Dachev V., Cherneva Z., 1979, *Longshore sediment movement at the Bulgarian Black Sea coast between c. Sivriburun and the Burgas Bay*, Oceanology (BAS, Sofia), 4, 30–41, (in Bulgarian).

Dachev V., Nikolov H., 1977, *Integral shore-line changes at accumulative sections between Cherni nos and Albena*, Oceanology (BAS, Sofia), 2, 57–64, (in Bulgarian).

Filippov A., 1988, *Prediction of longshore transport of suspended sediments (Bulgarian coast case study)*, Ph. D. thesis, Southern Branch of P. P. Shirshov Inst. Oceanol. RAS, (in Russian).

Longinov V., 1966, *Energy method for estimation of longshore movement of sediments in the coastal zone*, Proc. Soyuzmorniiproekt, Transport, 12 (18), 13–26.

Nikolov H., 1981, *The thickness of the dynamic layer and tendencies in the variation of the profile in front of the beach strips of the resort complex 'Albena', 'Zlatni Pyasatsi' and 'Druzhba'*, Oceanology (BAS, Sofia), 8, 60–75, (in Bulgarian).

Nikolov H., Keremedchiev S., 1993, *State-of-the-art and dynamic of some beaches of the Bulgarian Black Sea coast*, [in the part:] *Coastlines of the Black Sea*, 8th Symp. 'Coastal and Ocean Management', 19–23 July, Hyaff Regency, New Orleans, Louisiana, 508–530.

Nikolov H., Mutafova M., 2001, *Some negative trends in the development of the underwater slope in front of the beach of camp Europe*, Proc. Inst. Oceanol. BAS, Vol. 3, 99–104, (in Bulgarian).

Ozhan E., Abdalla S., Yilmaz N., 2005, *Long-term and extreme wave climate of the Black Sea*, Proc. 29th ICCE, Vol. 1, 701–713.

Pruszak Z., Ostrowski R., Skaja M., Szmytkiewicz M., 2000, *Wave climate and large-scale coastal processes in terms of boundary conditions*, Coast. Eng., 42 (1), 31–56.

Shore Protection Manual, 1984, US Army Coast. Eng. Res. Center.

Shuysky Y., Popov V., 1975, *Sediment fluxes along the Bulgarian Black Sea coastal zone*, Probl. Geogr., 43–47, (in Bulgarian).

Szmytkiewicz M., 2002a, *Quasi 3D model of wave-induced currents in coastal zone*, Arch. Hydro-Eng. Environ. Mech., 49 (1), 57–81.

Szmytkiewicz M., 2002b, *Wave-induced currents in the coastal zone*, IBW PAN, Gdańsk, 235 pp., (in Polish).

Szmytkiewicz M., Biegowski J., Kaczmarek L. M., Okrój T., Ostrowski R., Pruszak Z., Różyński G., Skaja M., 2000, *Coastline changes near harbour structures: comparative analysis of one-line models versus field data*, Coast. Eng., 40 (2), 119–139.

Trifonova E., 2005, *Model for wave refraction in shallow water*, Proc. Inst. Oceanol. BAS, Vol. 5, 91–101, (in Bulgarian).

Thornton E., 1970, *Variation of longshore current across the surf zone*, Proc. 12th ICCE, Vol. 1, 291–308.

UNIBEST-LT (Uniform Beach Sediment Transport – Longshore Transport), 1993, *Computations of sediment transport along a uniform coast. User's manual, version 4.0*, Delft Hydraulics.

Van Rijn L. C., 1993, *Principles of sediment transport in rivers, estuaries and coastal seas*, Aqua Publ., Amsterdam, 614 pp.